

# A Geometric Approach to Motion Control of a Standard Tractor-trailer Robot

Avinesh Prasad

School of Computing, Information  
and Mathematical Sciences  
University of the South Pacific  
Fiji  
Email: avinesh.prasad@usp.ac.fj

Bibhya Sharma

School of Computing, Information  
and Mathematical Sciences  
University of the South Pacific  
Fiji  
Email: bibhya.sharma@usp.ac.fj

Jito Vanualailai

School of Computing, Information  
and Mathematical Sciences  
University of the South Pacific  
Fiji  
Email: vanualailai@usp.ac.fj

**Abstract**—In this paper, we use a simple geometric approach to control the motion of a standard tractor-trailer robot from some initial positions to a goal position. The solution to the motion control problem is proposed in two steps. Firstly, the control laws are proposed that can drive the robot to a goal position whilst observing the mechanical singularities associated with the system. Secondly, the control laws are adjusted so that the robot can avoid any number of fixed obstacles in the workspace and safely reach the goal position. The proposed algorithm is verified using computer simulations.

**Index Terms**— Standard Tractor-trailer robot, nonholonomic, target convergence, obstacle avoidance.

## I. INTRODUCTION

A tractor-trailer system consists of a tractor towing an arbitrary number of trailers [1]. A common example in Fiji is the railway locomotive system used for transporting cane to the mill. The trailers are mostly passive so that the overall implementation and operational costs is reduced. The two different trailer systems found in literature are *standard* and the *general* trailer systems. The major difference between the two types is based upon the hooking schemes of the trailers. In a standard trailer system, a two-wheeled passive trailer is hitched directly on the midpoint of the rear axle of the tractor robot followed by any additional trailers hitched on the midpoint of the rear axle of the preceding trailer. In contrast, for the general trailer system, each trailer is hitched at a distance away from the midpoint of the rear axle of the preceding trailer / tractor. The reader can refer to [2] for a detailed explanation of the two trailer systems.

Tractor-trailer vehicles are mainly used in transportation industries [3] to carry load from one point to another. Prominent places include airports, wharfs, farms, mines to name a few and in environments that are harsh, hazardous or inaccessible to humans [1]. A tractor

trailer system will obviously operate at a low cost for goods transportation and concurrently save time and energy [4]. In fact, such systems can successfully complete a given task in a faster, cheaper and convenient way when compared to individual robots [3]. Example, a locomotive system transporting cane to crushing mills from a long distance when compared to multiple trucks.

The tractor robot and the passive trailers are all non-holonomic in nature. Due to the amalgamation of the nonholonomic structures, the kinematics of tractor trailer robot are complicated, nonlinear, underactuated, and subjected to nonholonomic constraints [5], [6]. The motion of the articulated robot is further restricted because of the associated mechanical singularities [1]. Another limitation associated with the movement of the multi-body system is the amount of space it takes during turning. Such system can face problems on narrow roads and bridges where the safety of the robot is of high priority [4]. Furthermore, if the workspace contains fixed or moving obstacles, the motion control problem becomes more difficult and challenging [2]. In literature, researchers have used various approaches to solve the motion control problem of tractor-trailer systems. Some prominent ones are H-infinity control approach [7], a fuzzy control approach [8], [9], a Lyapunov-based approach [1], [2], to name a few.

In this paper, we will use the idea proposed in [10] to control the motion of a standard tractor-trailer robot in a priori known workspace containing fixed obstacles. For simplicity we have considered circular and line obstacles of random sizes and positions. In [10], Prasad *at. al* proposed a unique and tailored technique for controlling the motion of a car-like robot in an obstacle ridden workspace. A velocity algorithm was developed and the steering angle modelled using neural network so that the car-like robot avoids obstacles and safely reach its goal position. The method used in [10] was systematic, elegant, straight forward and simple compared to

other methods, for example, the Lyapunov-based control scheme [1], [2] where there is no definite and standard procedure of constructing a Lyapunov function from which the controllers are extracted. We adopt the same technique and show that it can be applied to control the motion of a standard tractor-trailer robot.

The remainder of the paper is organized as follows. In Section II, the kinematic model of the standard tractor-trailer robot and the associated holonomic constraints are given. In Section III, the definition of the target and the system's mechanical singularities are given. The control laws for target convergence and adherence to the mechanical singularities is proposed. Section IV considers fixed obstacles and a collision-free algorithm is proposed where the robot moves safely from an initial position to its target position. Section V provides a summary on the contributions and lists the future work.

## II. KINEMATIC MODEL

We consider a standard tractor-trailer robot which is comprised of a rear wheel driven car-like vehicle and a hitched two-wheeled passive trailer attached to the rear axel of the vehicle. The standard 1-trailer system, adopted from [1], is shown in Figure 1.

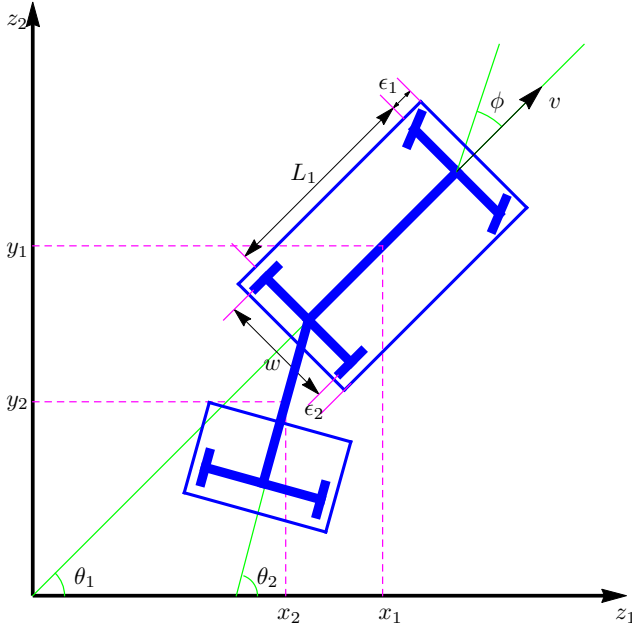


Fig. 1. The schematic representation of a standard 1-trailer robot (adopted from [1]).

Referring to Figure 1,  $(x_1, y_1)$  represents the cartesian coordinates of the tractor robot,  $\theta_1$  gives its orientation

with respect to the  $z_1$ -axis, while  $\phi$  gives the steering angle with respect to its longitudinal axis. Similarly,  $(x_2, y_2)$  represents the cartesian coordinates of the passive trailer while  $\theta_2$  gives its orientation with respect to the  $z_1$ -axis.

Letting  $L_1$  and  $L_2$  be the lengths of the mid-axle of the tractor and trailer, respectively, the kinematic model of a standard 1-trailer system, adopted from [1], is given by

$$\left. \begin{aligned} \dot{x}_1 &= v \cos \theta_1 - \frac{v}{2} \tan \phi \sin \theta_1, \\ \dot{y}_1 &= v \sin \theta_1 + \frac{v}{2} \tan \phi \cos \theta_1, \\ \dot{\theta}_1 &= \frac{v}{L_1} \tan \phi, \\ \dot{\theta}_2 &= \frac{v}{L_2} \sin (\theta_1 - \theta_2), \end{aligned} \right\} \quad (1)$$

where  $v$  is the translational velocity of the tractor robot. Note that we can express the position of the trailer completely in terms of the state variables  $x_1, y_1, \theta_1$  and  $\theta_2$  as follows:

$$\begin{aligned} x_2 &= x_1 - \frac{L_1}{2} \cos \theta_1 - \frac{L_2}{2} \cos \theta_2, \\ y_2 &= y_1 - \frac{L_1}{2} \sin \theta_1 - \frac{L_2}{2} \sin \theta_2. \end{aligned}$$

These position constraints, known as the holonomic constraints of the system, will reduce the dimension of the configuration space [2].

We further note that since we are considering a passive trailer, there is no need to impose any additional controller for  $\theta_2$ , hence the only controllers in system (1) are  $v(t)$  and  $\phi(t)$ . However, we need to observe any mechanical singularities associated with the movement of the trailer.

## III. MOTION CONTROL IN THE ABSENCE OF FIXED OBSTACLES

Our objective is to control the motion of the standard tractor-trailer robot to a designated goal position while observing any restrictions placed on the system due to mechanical singularities. We therefore designate a target (goal position) for the robot which is a disk of center  $(p_1, p_2)$  and radius  $r_T$ . The target is described as

$$T = \{(z_1, z_2) \in \mathbb{R}^2 : (z_1 - p_1)^2 + (z_2 - p_2)^2 \leq r_T^2\}.$$

We shall use the vector notation  $\mathbf{x}(t) = (x_1(t), y_1(t))$  to describe the position variables in (1) and  $\mathbf{e} = (p_1, p_2)$  to describe the goal position for  $\mathbf{x}(t)$ . For  $\mathbf{x}(t) \neq \mathbf{e}$ , we further define  $\xi(t)$  be the angular position of  $T$  with respect to the current position of the vehicle at time  $t$ . The angle  $\xi(t)$  is defined implicitly as

$$\tan \xi(t) = \begin{cases} \frac{p_2 - y_1(t)}{p_1 - x_1(t)}, & \text{if } \mathbf{x}(t) \neq \mathbf{e}; \\ \tan \xi(t-1), & \text{if } \mathbf{x}(t) = \mathbf{e}. \end{cases}$$

### A. Target Convergence

We want the tractor-trailer robot to start from an initial configuration, move towards its target and converge at the center of the target.

For the robot to maneuver from its initial position to the goal position, we shall adopt the velocity algorithm (modified from [10]):

$$v(t) = \alpha \|\mathbf{x}(t) - \mathbf{e}\|, \quad (2)$$

where  $\alpha > 0$  is a user-defined constant.

### B. Mechanical Singularities

There are two mechanical singularities associated with the system:

- Restrictions on the movement of the trailer.
- Restrictions on the steering angle  $\phi(t)$ .

Firstly, the motion of the trailer is restricted in the sense that the mid axle of the trailer should not collide with the rear axle of the vehicle [1]. That is, the angle  $\theta_2$  is restricted as

$$|\theta_2 - \theta_1| < \pi/2.$$

In order to adhere to this restriction, we treat the line passing through the points  $(x_1 - \frac{L_1}{2} \cos \theta_1 - \frac{L_2}{2} \sin \theta_1, y_1 - \frac{L_1}{2} \sin \theta_1 + \frac{L_2}{2} \cos \theta_1)$  and  $(x_1 - \frac{L_1}{2} \cos \theta_1 + \frac{L_2}{2} \sin \theta_1, y_1 - \frac{L_1}{2} \sin \theta_1 - \frac{L_2}{2} \cos \theta_1)$  as an artificial obstacle for the trailer. The trailer should always avoid this line during the motion. The distance from  $(x_2, y_2)$  to the closest point on the line is calculated to be  $R_0 = \frac{L_2}{2} \cos |\theta_1 - \theta_2|$ . We see that as  $|\theta_1 - \theta_2| \rightarrow \pi/2$ ,  $R_0 \rightarrow 0$ . Thus carefully including  $R_0$  into the controller  $\phi(t)$  will guarantee the adherence placed on the trailer.

Secondly, we note that the steering angle of the front wheel is bounded according to the inequality [2]

$$|\phi(t)| \leq \phi_{\max} < \frac{\pi}{2}.$$

where  $\phi_{\max}$  is maximum steering angle. Using the idea proposed in [10] and taking into account the restrictions on the movement of the trailer, we propose the following form of the controller  $\phi(t)$ :

$$\phi(t) = \frac{2\phi_{\max}}{\pi} \tan^{-1} \left( \xi(t) - \theta_1(t) + \frac{\alpha_0 \beta_0}{R_0} \right), \quad (3)$$

where

$$\alpha_0 = \begin{cases} 0, & \text{if } R_0 \geq w/2 \\ w/2 - R_0, & \text{if } R_0 < w/2 \end{cases} \quad \text{and}$$

$$\beta_0 = \begin{cases} -1, & \text{if } (y_2 - y_1) \cos \theta_1 - (x_2 - x_1) \sin \theta_1 \geq 0 \\ 1, & \text{if } (y_2 - y_1) \cos \theta_1 - (x_2 - x_1) \sin \theta_1 < 0 \end{cases}$$

*Simulation 1:* The nonlinear differential equations given in system (1) was numerically integrated using a fourth order Runge-Kutta method and the trajectories were plotted as shown in Figures 2 and 3. In each scenario the robot maneuvers from an initial to a final configuration, whilst maintaining the mechanical singularity restrictions. Table I gives the values of the different parameters used in the two simulations.

TABLE I  
VALUES OF THE DIFFERENT PARAMETERS USED IN THE SIMULATIONS.

Initial and Final Configuration	
Initial and final position	Refer to the Figures.
Initial orientation	Figure 2: $\theta_1 = \pi/4$ rad, $\theta_2 = 0$ rad. Figure 3: $\theta_1 = \pi/2$ rad, $\theta_2 = \pi/4$ rad.
Robot Parameters	
Dimensions	$L_1 = 3$ m, $w = 1.4$ m, $L_2 = 3$ m.
Safety parameters	$\epsilon_1 = 0.2$ m, $\epsilon_2 = 0.1$ m.
Other Parameters	
Workspace dimensions	$0 \leq z_1 \leq 50, 0 \leq z_2 \leq 50$ .
Constants	$\alpha = 0.05, \phi_{\max} = \frac{7\pi}{18}$ .

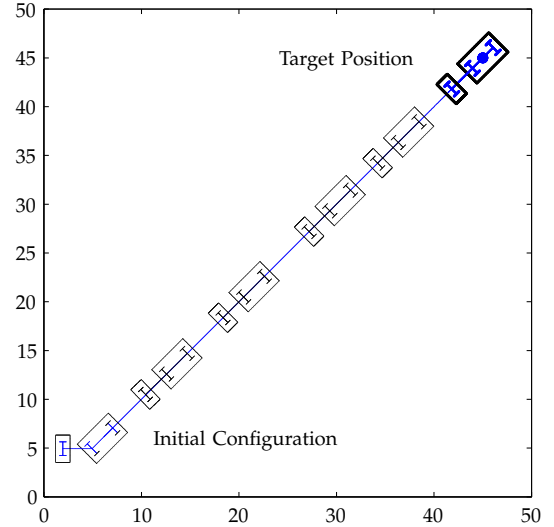


Fig. 2. Trajectory of the tractor-trailer robot with initial position (6, 6) and target position (45, 45)

## IV. MOTION CONTROL IN THE PRESENCE OF FIXED OBSTACLES

We now assume that the workspace is cluttered with stationary obstacles. The two types of obstacles considered in this paper are circular (disks) and line obstacles with *known* positions and sizes. To ensure that the entire vehicle safely steers pass any obstacle, we enclose the vehicle and the trailer by the smallest possible circles with centers and radii given in Table II. The constants  $\epsilon_1$  and  $\epsilon_2$  are the *clearance parameters* adopted from [2].

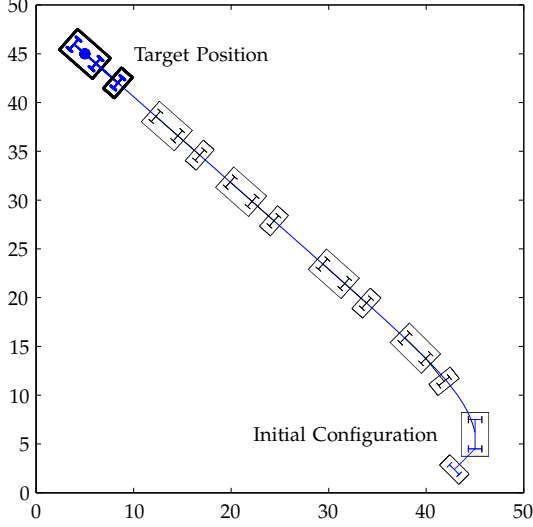


Fig. 3. Trajectory of the tractor-trailer robot with initial position (45, 6) and target position (5, 46)

TABLE II  
RADI AND CENTERS OF THE SMALLEST CIRCLES ENCLOSING EACH BODY.

Body	Center	Radius
Vehicle	$(x_1, y_1)$	$rv_1 = \frac{1}{2}\sqrt{(L_1 + 2\epsilon_1)^2 + (w + 2\epsilon_2)^2}$
Trailer	$(x_2, y_2)$	$rv_2 = \frac{1}{2}\sqrt{(L_2 + 2\epsilon_1)^2 + (w + 2\epsilon_2)^2}$

### A. Circular Obstacles

The  $l$ th circular obstacle with center  $(o_{l1}, o_{l2})$  and radius  $ro_l$  on the  $z_1z_2$  plane is defined as

$$FO_l = \{(z_1, z_2) \in \mathbb{R}^2 : (z_1 - o_{l1})^2 + (z_2 - o_{l2})^2 \leq ro_l^2\},$$

for  $l = 1, 2, \dots, q$ .

*Definition 1:* The set  $S$  defined by

$$S = \bigcup_{l=1}^q \{(z_1, z_2) \in \mathbb{R}^2 : (z_1 - o_{l1})^2 + (z_2 - o_{l2})^2 \leq (ro_l + d_{\max})^2\}$$

(where  $d_{\max} > 0$  is a predefined constant) is called the sensing zone.

The constant  $d_{\max}$  determines the size of the sensing zone. A large value of  $d_{\max}$  would mean that the robot avoids a fixed obstacle from a greater distance. We therefore regard  $d_{\max}$  as a *control parameter* in this paper.

In designing the control laws, we impose the following rules:

- 1) The robot should slow down when it approaches an obstacle.
- 2) The robot should change its direction when it enters the sensing zone.
- 3) The controllers should be continuous everywhere on its domain.

Keeping in mind the above rules, we propose the following forms of the controllers:

$$v(t) = \alpha \|\mathbf{x}(t) - \mathbf{e}\| \prod_{l=1}^q \left(1 - \frac{\alpha_l}{d_{\max}}\right),$$

$$\phi(t) = \frac{2\phi_{\max}}{\pi} \tan^{-1} \left( \xi(t) - \theta_1(t) + \sum_{l=0}^q \frac{\alpha_l \beta_l}{R_l} \right),$$

where

$$R_l = \min \left( \sqrt{(x_1 - o_{l1})^2 + (y_1 - o_{l2})^2} - rv_1, \sqrt{(x_2 - o_{l1})^2 + (y_2 - o_{l2})^2} - rv_2 \right) - ro_l,$$

$$f_l = (x_1 - o_{l1})(p_2 - y_1) - (y_1 - o_{l2})(p_1 - x_1),$$

$$\alpha_l = \begin{cases} 0, & \text{if } R_l \geq d_{\max} \\ d_{\max} - R_l, & \text{if } R_l < d_{\max} \end{cases} \quad \text{and}$$

$$\beta_l = \begin{cases} -1, & \text{if } f_l \geq 0 \\ 1, & \text{if } f_l < 0 \end{cases}$$

for  $l = 1, 2, \dots, q$ . We note that the factor  $\prod_{l=1}^q \left(1 - \frac{\alpha_l}{d_{\max}}\right)$  in  $v(t)$  will ensure that the robot would slow down as soon as it enters the sensing zone. The steering angle  $\phi(t)$  is inversely proportional to  $R_l$ . This would mean that when the robot comes close to an obstacle, the distance  $R_l$  will decrease. This will then increase  $|\phi(t)|$ , deviating the robot away from the obstacle.

*Simulation 2:* To illustrate the effectiveness of our proposed controllers, we have generated two trajectories of the tractor-trailer robot maneuvering from initial position and orientation to a goal position as shown in figures 4 and 5. In Figure 4, we have considered one circular obstacle centered at (28, 22) with radius 2. The robot with initial position (6, 6) and orientation  $\theta_1 = \theta_2 = 0$  maneuvers to its goal position at (45, 45) whilst avoiding the fixed obstacle along its route. The control parameter  $d_{\max} = 4$  was used while the robot parameters, workspace dimension,  $\alpha$  and  $\phi_{\max}$  are given in Table I.

In Figure 5, we have considered multiple circular obstacles with random positions and sizes. We again notice that the robot avoids all the fixed obstacle that lie on its route and safely converge to its goal position.

Figure 10 shows the graph of the controllers  $v(t)$  and  $\phi(t)$  for the trajectory shown in Figure 5. The controllers vanish when the robot reaches its goal position. We have

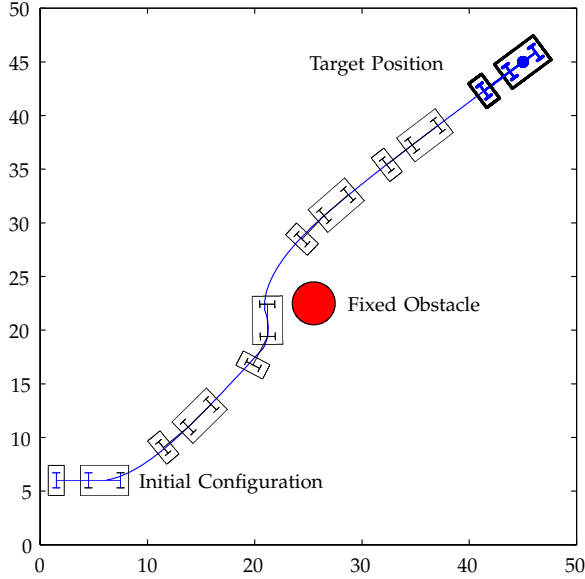


Fig. 4. Trajectory of the tractor-trailer robot in the presence of one fixed obstacle.

also generated the graph of  $\theta_2(t) - \theta_1(t)$  versus time,  $t$  as shown in Figure 7. From the graphs, we can clearly notice that restrictions ( $|\theta_2 - \theta_1| < \pi/2$  and  $|\phi(t)| \leq \phi_{\max}$ ) due to the mechanical singularities of the system is observed during the entire motion of the robot.

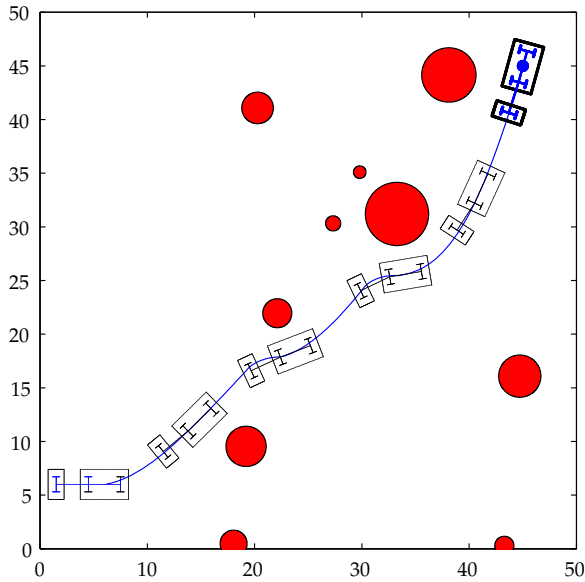


Fig. 5. Trajectory of the tractor-trailer robot in the presence of multiple fixed obstacle.

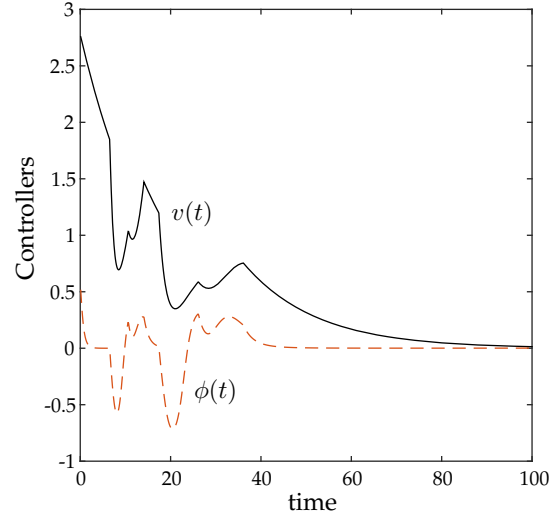


Fig. 6. Evolution of the controllers along the trajectory shown in Fig. 5.

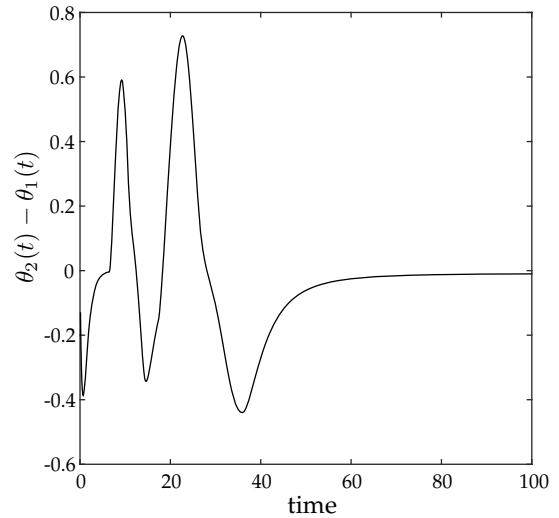


Fig. 7. Graph of  $\theta_2(t) - \theta_1(t)$  versus time for the trajectory shown in Fig. 5.

### B. Line Obstacles

Next, let us fix  $m > 0$  line obstacles in the workspace. In real-life situation, the line obstacles may be used to represent:

- boundaries of a rectangular workspace;
- sides of a polygonal obstacle;
- boundaries of a building;
- partitions of rooms inside a building;

- boundary lines of the parking bay [2].

The  $k$ th line segment in the  $z_1z_2$ -plane, from the point  $(a_{k1}, b_{k1})$  to the point  $(a_{k2}, b_{k2})$  is represented by the set

$$LO_k = \{(z_1, z_2) \in \mathbb{R}^2 : (z_1 - X_k)^2 + (z_2 - Y_k)^2 = 0\},$$

where  $X_k = a_{k1} + (a_{k2} - a_{k1})\lambda_k$  and  $Y_k = b_{k1} + (b_{k2} - b_{k1})\lambda_k$  is its parametric representation for  $0 \leq \lambda_k \leq 1$ .

For each body of the robot to avoid the  $k$ th line segment, we utilize the minimum distance technique (MDT). The reader can refer to [2] for detailed explanations on MDT. Minimizing the Euclidean distance between the point  $(x_i, y_i)$  and the point  $(X_{ik}, Y_{ik})$  on the  $k$ th line segment, we get

$$\lambda_{ik} = \frac{(x_i - a_{k1})(a_{k2} - a_{k1}) + (y_i - b_{k1})(b_{k2} - b_{k1})}{(a_{k2} - a_{k1})^2 + (b_{k2} - b_{k1})^2},$$

for  $i = 1, 2$ . We further note that the value of  $\lambda_{ik}$  should be between 0 and 1. Hence if  $\lambda_{ik} \geq 1$ , then we let  $\lambda_{ik} = 1$  and if  $\lambda_{ik} \leq 0$ , then we let  $\lambda_{ik} = 0$ .

For the tractor-trailer robot to avoid the line segments (as well as the circular obstacles), we define the controllers as

$$v(t) = \alpha \|\mathbf{x}(t) - \mathbf{e}\| \prod_{l=1}^q \left(1 - \frac{\alpha_l}{d_{\max}}\right) \prod_{k=1}^m \left(1 - \frac{\gamma_k}{d_{\max}}\right),$$

$$\phi(t) = \frac{2\phi_{\max}}{\pi} \tan^{-1} \left( \xi(t) - \theta_1(t) + \sum_{l=0}^q \frac{\alpha_l \beta_l}{R_l} + \sum_{k=1}^m \frac{\gamma_k \rho_k}{D_k} \right),$$

where

$$D_k = \min \left( \sqrt{(x_1 - X_{1k})^2 + (y_1 - Y_{1k})^2} - rv_1, \right. \\ \left. \sqrt{(x_2 - X_{2k})^2 + (y_2 - Y_{2k})^2} - rv_2 \right),$$

$$g_k = (x_1 - X_{1k})(p_2 - y_1) - (y_1 - Y_{1k})(p_1 - x_1),$$

$$\gamma_k = \begin{cases} 0, & \text{if } D_k \geq d_{\max} \\ d_{\max} - D_k, & \text{if } D_k < d_{\max} \end{cases} \quad \text{and}$$

$$\rho_k = \begin{cases} -1, & \text{if } g_k \geq 0 \\ 1, & \text{if } g_k < 0 \end{cases}$$

for  $k = 1, 2, \dots, m$ .

*Simulation 3:* Figures 8 and 9 show trajectories of the tractor trailer robot in two different workspace cluttered with various obstacles. In Figure 8, we have considered four line obstacles which forms a rectangular object for the robot to avoid on its way to the target. However, in Figure 9, we have considered two rectangular obstacles and a few circular obstacles of random sizes and positions. The initial and target positions are given in the graph captions. The control parameter  $d_{\max} = 4$  was used while the robot parameters, workspace dimension,  $\alpha$  and  $\phi_{\max}$  are given in Table I.

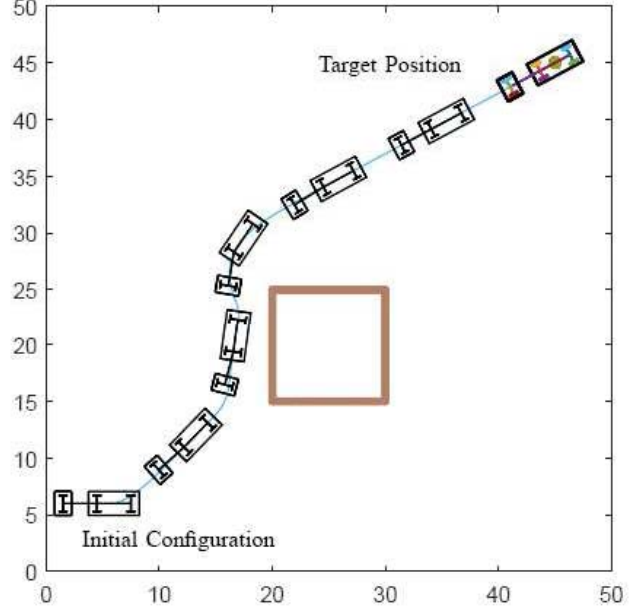


Fig. 8. Trajectory of the tractor-trailer robot avoiding a rectangular obstacle.

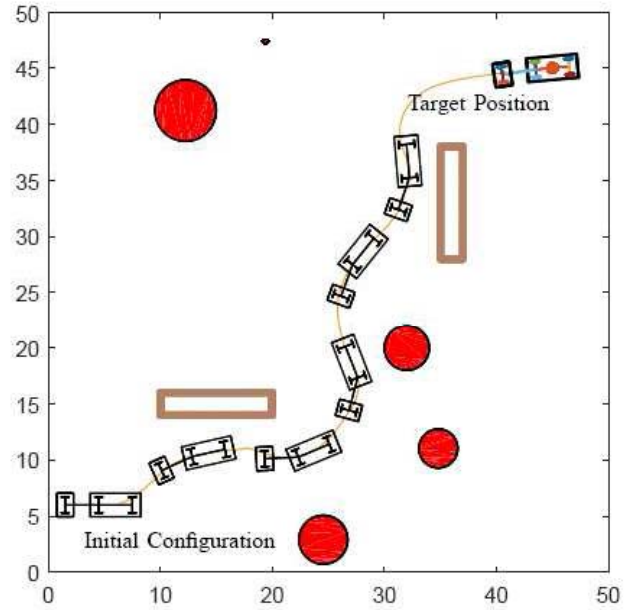


Fig. 9. Trajectory of the tractor-trailer robot avoiding rectangular and circular obstacles

Figure 10 shows the graph of the controllers  $v(t)$  and  $\phi(t)$  for the trajectory shown in Figure 9. As usual, the controllers vanish when the robot reaches its goal position.

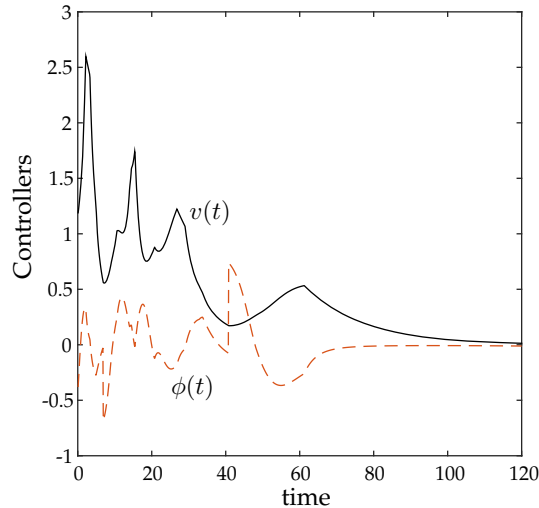


Fig. 10. Evolution of the controllers along the trajectory shown in Fig. 9.

## V. CONCLUSION

This paper presents a simple yet noble and unique technique to solve the motion control problem of a standard tractor-trailer robot. We first considered the motion of the robot in an obstacle-free workspace. The proposed controllers ensured that the robot maneuvers from initial to goal position while observing the mechanical singularity restrictions. Secondly, in the presence of fixed obstacles, the various obstacle parameters were included in the control laws which ensured that the robot slowed down on approach to an obstacle and safely deviate away without colliding.

The new control laws proposed in this paper ensure safe and smooth system trajectories and works for any number of fixed circular and line obstacles. Computer simulations are used to numerically verify the effectiveness of the proposed techniques.

Future work in this research area will involve attaining a desired final orientations of each body, inclusion of fixed and moving obstacles of various shapes such as elliptic and arc obstacles. Moreover, an unknown workspace, where the positions, sizes and geometry of obstacles are unknown, will be interesting but challenging.

## REFERENCES

- [1] B. Sharma, J. Vanualailai, K. Raghuwaiya, and A. Prasad. New potential field functions for motion planning and posture control of 1-trailer systems. *International Journal of Mathematics and Computer Science*, 3(1):45–71, 2008.
- [2] B. Sharma. *New Directions in the Applications of the Lyapunov-based Control Scheme to the Findpath Problem*. PhD thesis, University of the South Pacific, Suva, Fiji Islands, July 2008.
- [3] Jennifer David and P. V. Manivannan. Control of truck-trailer mobile robots: a survey. *Intelligent Service Robotics*, 7(4):245–258, 2014.
- [4] P. Ritzen, E. Roebroek, N. van de Wouw, Z. P. Jiang, and H. Nijmeijer. Trailer steering control of a tractor-trailer robot. *IEEE Transactions on Control Systems Technology*, 24(4):1240–1252, July 2016.
- [5] P. Svestka and J. Vleugels. Exact motion planning for tractor-trailer robots. In *Robotics and Automation, 1995. Proceedings., 1995 IEEE International Conference on*, volume 3, pages 2445–2450 vol.3, May 1995.
- [6] A. Keymasi Khalaji and S. A. A. Moosavian. Robust adaptive controller for a tractor-trailer mobile robot. *IEEE/ASME Transactions on Mechatronics*, 19(3):943–953, June 2014.
- [7] A. Dolly Mary, Abraham T. Mathew, and Jeevamma Jacob. A robust h-infinity control approach of uncertain tractor trailer system. *IETE Journal of Research*, 59(1):38–47, 2013.
- [8] Jin Cheng, Yong Zhang, and Zhonghua Wang. Backward tracking control of mobile robot with one trailer via fuzzy line-of-sight method. In *Proceedings of the 6th International Conference on Fuzzy Systems and Knowledge Discovery - Volume 4, FSKD'09*, pages 66–70, Piscataway, NJ, USA, 2009. IEEE Press.
- [9] M Abroshan, M Taiebat, A Goodarzi, and A Khajepour. Automatic steering control in tractor semi-trailer vehicles for low-speed maneuverability enhancement. *Proceedings of the Institution of Mechanical Engineers, Part K: Journal of Multi-body Dynamics*, 2016.
- [10] A. Prasad, B Sharma, and J. Vanualailai. A solution to the motion planning and control problem of a car-like robot via a single layer perceptron. *Robotica*, 32(6):935–952, 2014.